Towards Practical SERS Sensing

Yiping Zhao
Nanoscale Science and Engineering Center, Department of Physics and Astronomy, the University of Georgia, Athens, GA 30602

ABSTRACT

Since its discovery more than 30 years ago, surface-enhanced Raman scattering (SERS) has been recognized as a highly sensitive detection technique for chemical and biological sensing and medical diagnostics. However, the practical application of this remarkably sensitive technique has not been widely accepted as a viable diagnostic method due to the difficulty in preparing robust and reproducible substrates that provide maximum SERS enhancement. Here, we demonstrate that the aligned silver nanorod (AgNR) array substrates engineered by the oblique angle deposition method are capable of providing extremely high SERS enhancement factors ($>10^8$). The substrates are large area, uniform, reproducible, and compatible with general microfabrication process. The enhancement factor depends strongly on the length and shape of the Ag nanorods and the underlying substrate coating. By optimizing AgNR SERS substrates, we show that SERS is able to detect trace amount of toxins, virus, bacteria, or other chemical and biological molecules, and distinguish different viruses/bacteria and virus/bacteria strains. The substrate can be tailored into a multi-well chip for high throughput screening, integrated into fiber tip for portable sensing, incorporated into fluid/microfluidic devices for *in situ* real-time monitoring, fabricated onto a flexible substrate for tracking and identification, or used as on-chip separation device for ultra-thin layer chromatography and diagnostics. By combining the unique SERS substrates with a handheld Raman system, it can become a practical and portable sensor system for field applications. All these developments have demonstrated that AgNR SERS substrates could play an important role in the future for practical clinical, industrial, defense, and security sensing applications.

Keywords: Ag nanorods, oblique angle deposition, surface enhanced Raman scattering, chemical and biological detection

1. INTRODUCTION

Surface-enhanced Raman scattering (SERS) is a promising and powerful spectroscopic method for high sensitive analysis of chemical and biological agents.[1-3] Since its discovery in the 1970's,[4-6] this phenomenon has attracted enormous research attention, much of which has focused on developing SERS as a practical sensing technique for security and diagnostic applications.[7-15] A critical aspect of SERS related application is to develop a metallic surface of specific morphology to alter the local electric field and to achieve reproducible and high levels of enhancement. Some of the important requirements for an ideal SERS substrate in practical diagnostic applications are that the substrate 1) produces a high enhancement; 2) generates a reproducible performance; 3) provides a uniform response; 4) has a stable shelf-life; and 5) is simple and cheap to fabricate. For the past 30 years, large volumes of literature have been published that focus on how to achieve ideal SERS substrates, which has been coupled to the advance of nanofabrication techniques. So far, there are four different forms of SERS substrates that have been generally fabricated by various nanofabrication methods: (1) zero-dimensional (0D) nanoparticles (NPs), including particles with different size and shape, different structures such as core-shell NPs, cages, hollow particles, crescent-shaped particles, NP dimmers, trimers, etc; (2) one-dimensional (1D) nanorods (NRs) and nanowires (NWs), including metallic nanorods and wires, chains of nanoparticles, heteronanorods, etc.; (3) two-dimensional (2D) nanostructures, such as nanoparticle aggregates, regular 2D nanostructure arrays, nanoparticle thin films, nano-hole arrays, etc; and (4) three-dimensional(3D) nanostructures, such as fractal (dendrite) structures, nanoparticle 3D networks, porous network, nanorod arrays etc. Most of the SERS substrates are formed by a physical or chemical process, such as deposition, etching, aggregation, etc, with complicated preparation conditions. Unfortunately, many of these fabrication methods are either expensive or time consuming, and fail to produce reproducible substrates that provide high SERS enhancements.

So far, five fabrication techniques could potentially produce good SERS substrates and meet the above mentioned requirements: electron beam lithography, nanosphere lithography, template methods, hybrid methods and an oblique

Independent Component Analyses, Compressive Sampling, Wavelets, Neural Net, Biosystems, and Nanoengineering X, edited by Harold Szu, Liyi Dai, Proc. of SPIE Vol. 8401, 84010O · © 2012 SPIE · CCC code: 0277-786X/12/$18
doi: 10.1117/12.918761

angle vapor deposition method. The electron beam lithography (EBL) method is ideal to produce uniform and reproducible SERS substrates.[16-20] However, it is very expensive and time-consuming to produce large area substrates using EBL, unless it is combined with a nanoimprint lithography method.[21] The nanosphere lithography (NSL) method pioneered by Van Duyne and co-workers involves evaporating Ag on closely packed colloid particle monolayer arrays pre-deposited onto a substrate. The nano- or micro-spherical particles are then subsequently removed leaving behind the Ag metal selectively deposited within the interstices to form a regular Ag nanostructure array on the substrate.[22-29] The template method utilizes a nanotube-like array such as anodized aluminum oxide membranes as a template to directly deposit Ag or Au nanorods into the channels via an electrochemical plating method.[30-36] Hybrid methods fabricate SERS substrates by depositing metal particles onto nanoporous scaffolds such as porous silicon, nanorod arrays, etc.[37-44] Recently we have found that Ag nanorod array (AgNR) substrate fabricated by the so-called oblique angle deposition (OAD) method can serve as excellent SERS substrates.[45-47] We demonstrated that SERS Enhancement Factor (EF) of trans-1,2-bis(4-pyridyl)ethene (BPE) can reach as high as ~10^9 with appropriate Ag nanorod geometry. In this paper, we present a brief review on our current progress of AgNR SERS substrates fabricated by OAD. We focus on the optimization of the substrates, the potential commercialization and device fabrications, and different sensing applications.

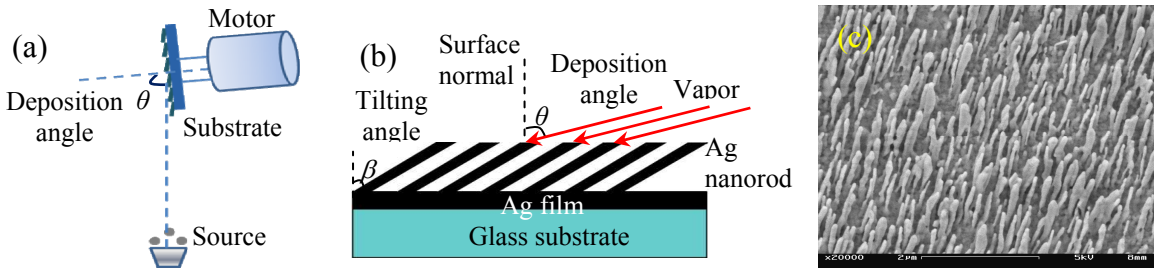

Fig. 1. (a) The schematic diagram of Ag nanorod array fabricated by oblique angle deposition; (b) the definition of deposition angle θ and Ag nanorod tilting angle β; and (c) a representative SEM image of the AgNR substrates (θ = 86°).

2. SILVER NANOROD SERS SUBSTRATES

2.1 AgNR fabrication and characterization

OAD is a physical vapor deposition technique in which the vapor atoms are deposited on a substrate at a large incident angle θ (> 70°) with respect to the surface normal of the substrate. Due to the shadowing effect and surface diffusion, nanocolumnar structures can be formed.[19-21] This technique has the following major advantages: the diameter, shape, spacing and density of the nanostructures can be easily controlled by changing deposition conditions such as the deposition angles, growth time, growth rate, and substrate temperature. For the OAD nanorods discussed in this paper, the AgNR arrays were deposited by a custom–designed electron-beam evaporation system. Figure 1(a) shows a schematic diagram of Ag nanorod array fabricated by OAD, and Figure 1(b) illustrates a general structure of the AgNR film. An underlayer thin film (such as Ag, Si, Ti) with fixed thickness was first deposited onto the cleaned glass substrates. During the evaporation, the thickness of the metal deposited was monitored by a quartz crystal microbalance positioned at normal incidence to the vapor source. The base pressure was around 8.6 × 10^{-7} Torr, and the Ag (Alfa Aesar, 99.999%) growth rate was 0.3 nm/s. The morphologies of as-deposited samples were characterized by a field-emission scanning electron microscope (SEM) (FEI Inspect F). Due to the shadowing growth mechanism, the OAD deposition results in arrays of Ag nanorods tilting towards the source material. The Ag nanorod tilting angle β is defined as the angle between the Ag nanorod tilting direction and substrate surface normal as shown in Fig. 1(b), and can be characterized using the cross-sectional SEM images. For SERS characterization, the Raman probe molecule, trans-1,2-bis (4-pyridyl) ethylene (BPE, Aldrich, 99.9+%) was used, and a 1 μL droplet of BPE methanol solution with a concentration of 10^{-5} M was dispensed on the surface of Ag nanorod arrays. After the droplet was dried, the spreading area was observed to be about 1 cm^2 for all the substrates. The Raman spectra were recorded by the HRC-10HT Raman Analyzer from Enwave Optronics Inc, with the excitation wavelength 785 nm, the power of 21 mW, the diameter of the laser spot 0.1 mm, and the collection time 10 s. To obtain the SERS enhancement factor, normal Raman spectra were measured from BPE methanol bulk solution with a concentration of 10^{-2} M contained in the quartz rectangular cuvette with a path length of 1 mm.

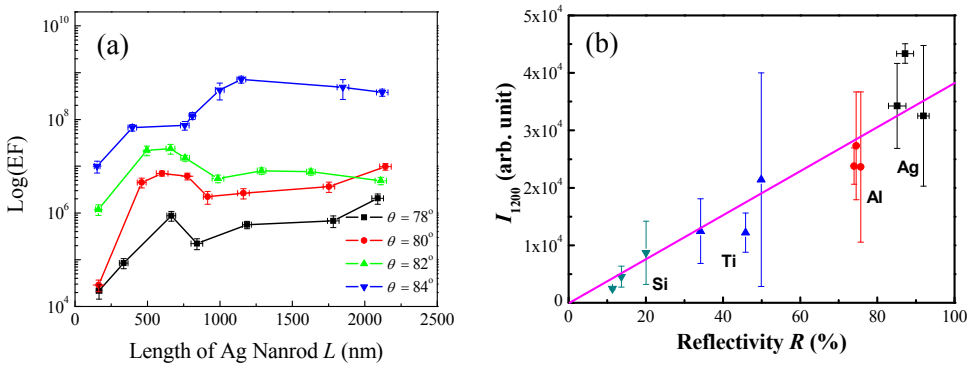

Fig. 2. (a) The SERS EF as a function of nanorod length L for samples deposited $\theta = 78°$, 80°, 82°, and 84°, respectively; and (b) the SERS peak intensity I_{1200} as a function of reflectance from the underlayer.

2.2 AgNR SERS substrate optimization

The morphology of the AgNRs plays an important role on the SERS performance. A systematic study has been carried out to explore the optimal AgNR structures for SERS application.[47] Here we first studied how the length, tilting angle and nanorod density affecting SERS of AgNRs. The underlayer thin film was fixed as a 500-nm Ag film, and a AgNR array layer was prepared by OAD technique at different deposition angles $\theta = 78°$, 80°, 82°, and 84°, respectively. For each deposition angle, there were 8 samples with different lengths deposited. Figure 2(a) plots the experimentally obtained SERS EF as a function of nanorod length L for Ag nanorod samples prepared at different lengths. For different deposition angles, the SERS EF also shows strong length dependence with a similar trend: the EF first increases with the nanorod length L, reaches a maximum at an optimum length L, and then decreases with further increase of length L. More specifically, for $\theta = 78°$, $L < 200$ nm, the EF is relatively low (~10^4). The EF reaches a maximum value of 8.7×10^5 when $L = 660$ nm, and then decreases slightly, and then increases to 2.0×10^6 when $L = 2100$ nm. For $\theta = 80°$, the EF-L relationship follows the same trend of that for $\theta = 78°$. The EF reaches a maximum value of 7.0×10^6 when $L = 600$ nm and 9.8×10^6 when $L = 2100$ nm. For $\theta = 82°$, the EF reaches a maximum value of 2.4×10^7 when $L = 660$ nm. For $\theta = 84°$, the maximum EF value is 7.2×10^8 when $L = 1100$ nm. For all the samples, the SERS EF obtained from samples prepared at $\theta = 84°$ is apparently much larger than those deposited at $\theta = 78°$, 80°, and 82°.

The AgNR arrays must be deposited onto a supporting substrate to show the large SERS EF. We have found that the optical properties of the under layer substrate also play a significant role in determining the SERS response of those Ag NR substrates.[48] For the standard AgNR SERS substrates, the underlayer is a 500 nm Ag thin film on 20 nm Ti-coated glass. In order to investigate the underlayer effect, thin films with different thickness and four different materials (Ag, Si, Ti, and Al) were prepared. After depositing the underlayers, the reflectance spectra from these underlayers were measured using a UV-Vis 2450 spectrometer system with an integration sphere (Shimadzu). Then, a ~ 900 nm Ag nanorod array deposited at $\theta = 86°$ onto these different underlayer films under the same deposition conditions. The SERS response of BPE under the same sample preparation conditions and SERS measurement conditions are obtained. Figure 2(b) show the how the SERS intensity of 10^{-5} M BPE signal changes versus the surface reflection at $\lambda = 350$ nm. We found that the SERS intensity increases monotonically with the reflectance from the underlayer at excitation wavelength 785 nm.

2.3 Engineering three-dimensional AgNR arrays

Folding straight AgNRs into zig-zag structures could generate corners or bends that become potential "hot spots" for SERS.[49, 50] The "hot spots" are locations with extremely high local electric fields. Using the dynamic shadowing growth method (azimuthal rotation during deposition), zig-zag AgNR arrays with different bending number N and fixed total rod length are fabricated (Fig. 3 (a)-(h)), and their SERS performance based on Rhodamine 6G are measured and compared (Fig. 3 (i) and (j)). The SERS intensity increases with N when $N < 4$, and decreases when $N > 4$. Since the total nanorod lengths are the same, the SERS intensity of zig-zag AgNR arrays with different N is determined by the

amount of "hot spots" when $N < 4$. The results suggest that folding AgNRs into three-dimensional structures is a promising way to design highly sensitive SERS substrates.

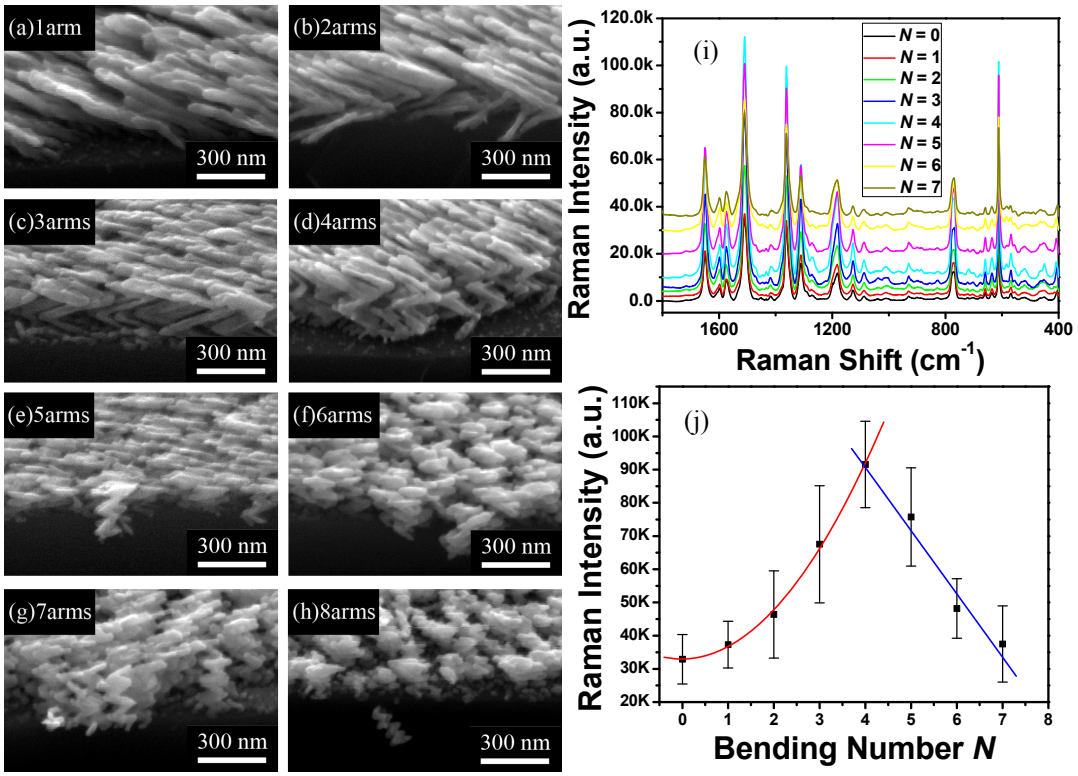

Fig. 3. (a)-(h) The representative SEM images of bent AgNR with different numbers of bending arms; (i) the SERS responses of the 3D substrates; and (j) the SERS intensity versus the number of bends.

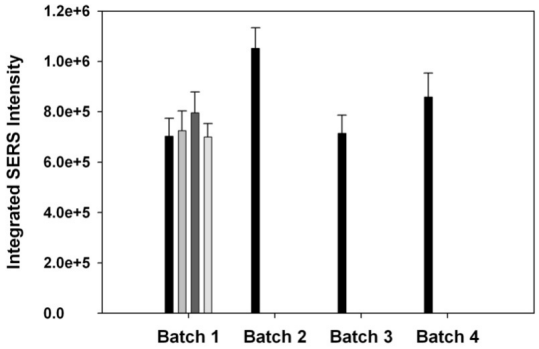

Fig. 4. Integrated intensity of the BPE band centered at 1200 cm^{-1}. Each bar represents the average intensity collected from five random locations on a single substrate and the error bars represent the standard deviation.

2.4 SERS signal uniformity and reproducibility of AgNR SERS substrates

The uniformity of the 1 cm × 1 cm AgNR SERS substrates was previously evaluated with respect to: i) the uniformity of SERS intensity across a single substrate, ii) the repeatability of the SERS signal collected from different substrates prepared in the same deposition batch, and iii) the reproducibility of the SERS signal from substrates prepared in different batches. Detailed discussion of this investigation is provided elsewhere;[46, 51] however, a summary of the results are provided in Figure 4. Ultimately, the spot-spot variation in signal ranged from 8-11%, substrate-to-substrate variation in signal ranged from 6-13% for substrates prepared in the same batch, and batch-to-batch variability was

determined to be <15%. This reproducibility is comparable to SERS substrates prepared with state-of-the-art EBL fabrication methods (20% RSD)[52] and is suited for quantitative studies.

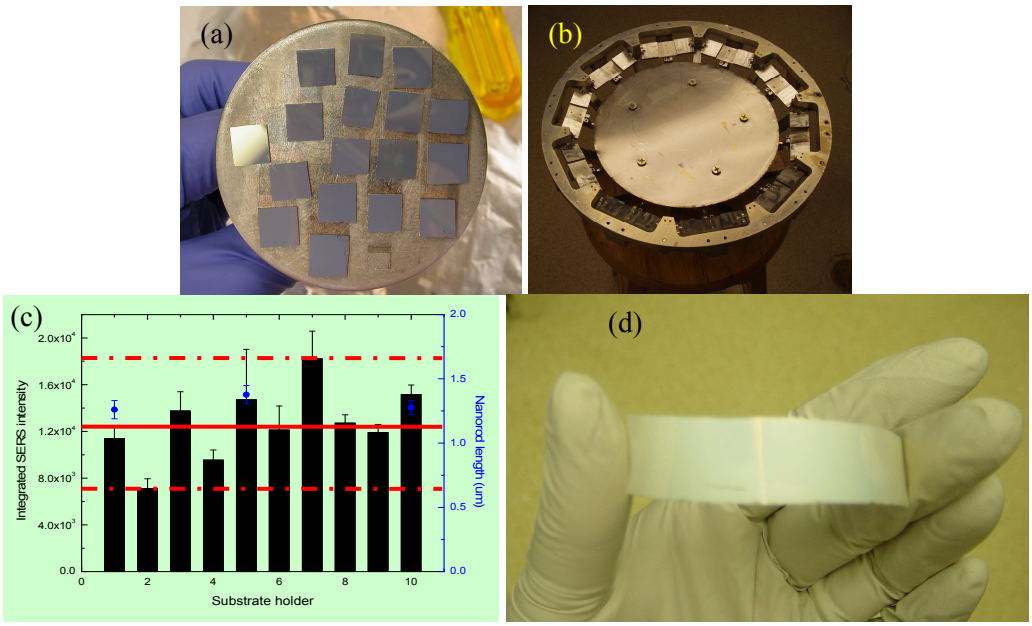

Fig. 5. Large scale AgNR SERS substrate fabrication: (a) multiple 1 cm × 1 cm samples on a 3”-diamter substrate holder; (b) special substrate holder designed to hold 10 1” × 3” glass slide substrates; (c) the SERS response of the 10 1” × 3” substrates; and (d) flexible SERS substrate: AgNR arrays on PET film.

3.SERS BASED LARGE SCALE FABRICATION AND DEVICES

3.1 Large scale SERS substrate production

Since the OAD method is a physical vapor deposition method, it is a large scale production technique used for surface coating. It is very easy to use OAD method to produce a large quantity of small area SERS substrates, which is difficult for other SERS substrate fabrication techniques. For example, Figure 5(a) shows that a 3”-diameter conventional substrate holder in an electron beam evaporation system can produce at least 17 1 cm × 1 cm AgNR SERS substrates. Clearly if we use slightly larger substrate holder with tightly arranged substrates, it is very easy to produce 40-50 uniform 1 cm × 1 cm substrates in one deposition. Also, a special umbrella-like multiple substrate holder can be designed to simultaneously load 10 1” × 3” or 2” × 3” glass slide substrates and perform AgNR substrate fabrication (Fig. 5(b)). The substrate holder is rotated while centered around the vapor incident beam direction to guarantee uniform deposition. The SERS responses of the 10 substrates are shown in Fig. 5(c). Since the AgNR fabrication only uses a room temperature substrate holder, the limitation of use of different types of substrate materials will be less stringent compared to other SERS substrate fabrication techniques. One can place plastic substrates such as polyethylene terephthalate (PET) or polydimethylsiloxane (PDMS) flexible films onto the substrate holder and make flexible SERS substrates. Figure 5(d) shows one example of the PET SERS substrates. These disposable and flexible SERS substrates can be integrated with biological substances and offer a novel and practical method to facilitate biosensing applications.

3.2 Multi-well SERS chip

The unique OAD process can produce large area uniform AgNR SERS substrates as shown in Fig. 5, which means one could confine the sensing the area into small wells in order to obtain better uniformity and sensitivity while reducing the amount of substrate used. We can employ a molding process to obtain multi-well SERS substrate on a 1”×3” SERS substrate as shown in Fig. 6.[51] The SERS substrate was loaded into an aluminium mold designed to create a 4×10 array of SERS active sample areas. PDMS was injected into the mold and cured at 100 ˚C for 25 minutes to form the wells on the surface of the SERS substrate. Each well has a diameter of 4 mm and height of 1 mm (Fig. 6). Details of the

mold and molding process has been previously reported.[51] This design confines the samples to a defined sensor area and facilitates the simultaneous screening of 40 samples. The responses of the 40 wells are very uniform, and the SERS signal fluctuation is within 20%.

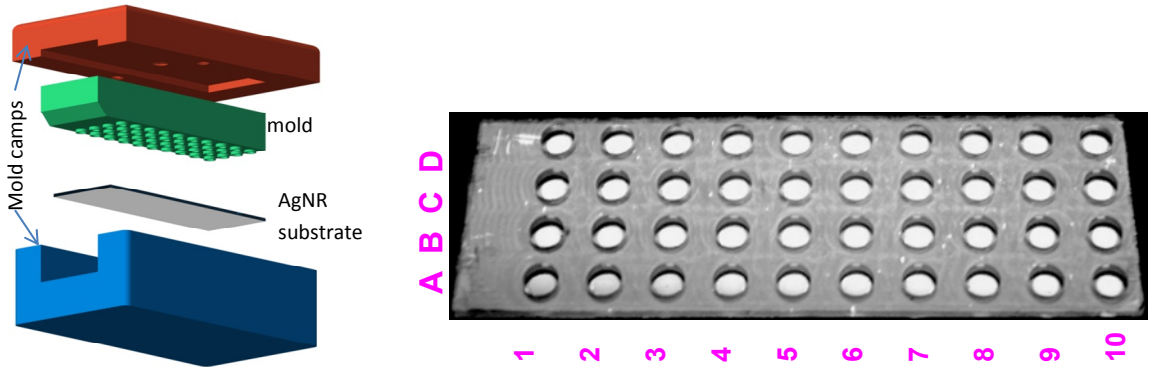

Fig. 6. A molding process to produce multi-well SERS chip and the resulting chip.

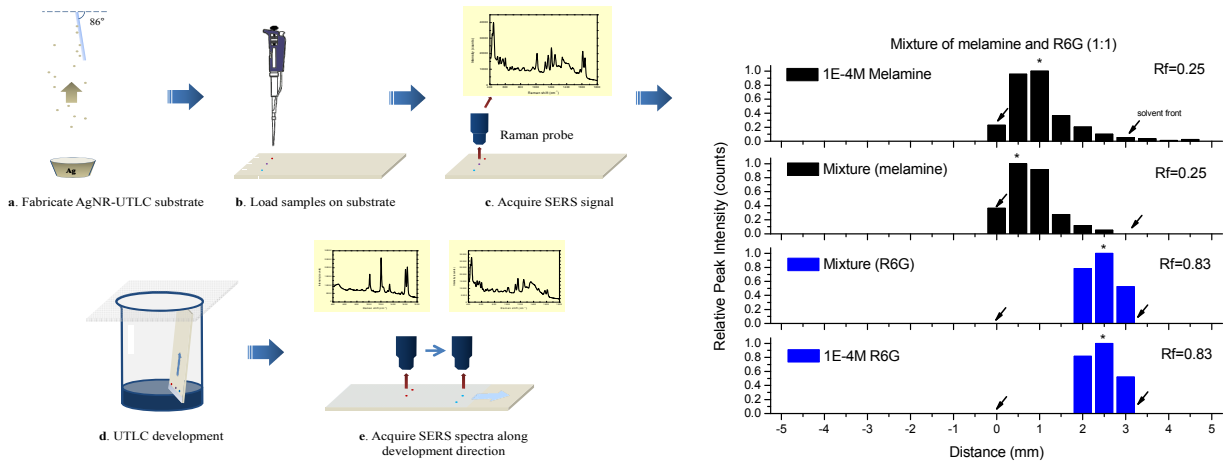

Fig. 7. The SERS-TLC process on a uniform AgNR substrate, and the separation and detection of a mixture of melamine and R6G.

3.3 On-chip separation and detection

The AgNR arrays SERS substrates have the unique anisotropic nanoporous structures with the nanorod diameters under 100 nm in at least two dimensions, and can be directly use as a separation device for ultra-thin layer chromatography (UTLC).[53] Because the AgNR film is SERS-active, the chip can also be used simultaneously as a detection or diagnostic device. Such a unique on-chip separation and detection capability make the AgNR chip closer for practical application. Fig. 7 shows a general procedure for SERS-UTLC process. This device has been tested for melamine-dye separation. The chromagraphs of melamine and R6G of 1:1 mixture of melamine and R6G using their spatially resolved unique Raman peaks were obtained and compared to the chromagraphs of the pure melamine and pure R6G solutions (Fig. 7). Even the melamine SERS signal dominate the mixture's SERS spectra, after TLC, one can clearly resolve the R6G signals.

3.4 Fiber SERS probes

By designing a special substrate holder, one can deposit AgNR arrays directly onto a polished fiber tip or on the outer surface of a tapered fiber as shown in Fig. 8.[54] Once these AgNRs are coated on fiber tips and integrated into a Raman system, they can be used as remote sensing probes as shown in Fig. 8.

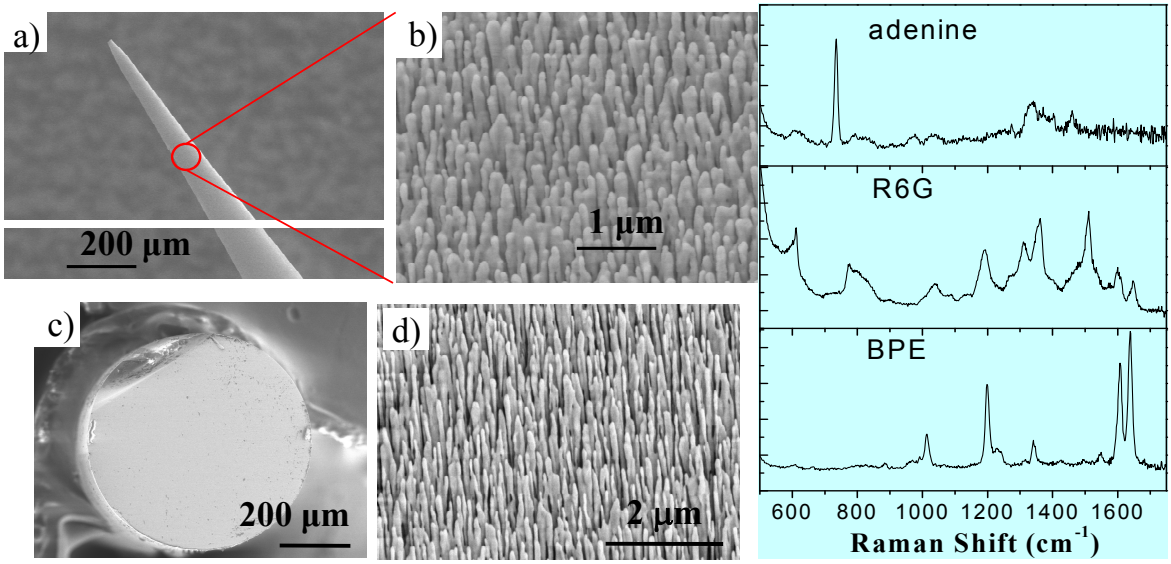

Fig. 8. The representative SEM images of AgNR arrays on taped fiber tip and polished fiber end and the measured SERS responses of different analytes using the AgNR coated fiber tips.

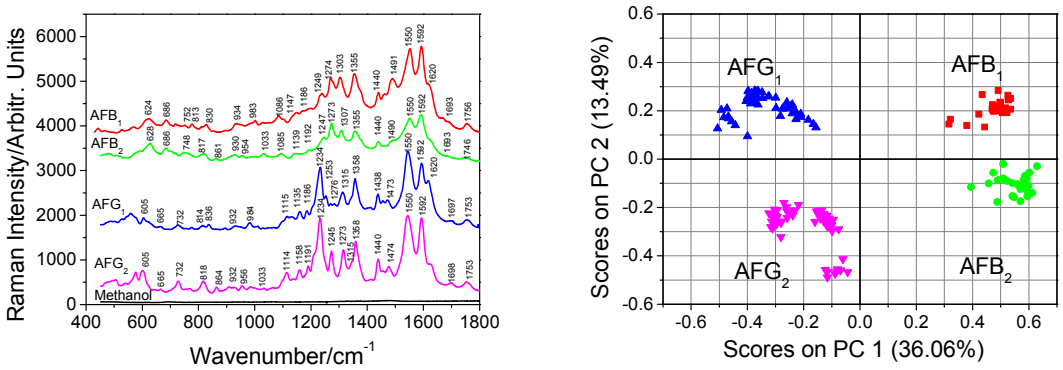

Fig. 9. The SERS spectra of four AFs and the PCA score plot.

4. SENSING APPLICATIONS

4.1 Toxins

Aflatoxins (AFs) are a group of hepatotoxic, carcinogenic, mutagenic, and teratogenic mycotoxins mainly produced by *Aspergillus flavus*, *A. parastiticus* and *A. nomius*.[55] There are four major AFs, AF B_1 ($C_{17}H_{12}O_2$), B_2 ($C_{17}H_{14}O_6$), G_1 ($C_{17}H_{12}O_7$), and G_2 ($C_{17}H_{14}O_7$), that naturally occur in food commodities. Among them, aflatoxin B_1 (AFB_1) has the most potent toxicity and carcinogenicity to animals and human, and it has been recognized as a group I carcinogen by the International Agency for Research on Cancer (IARC),[56] due to the evidences of its ability to cause malignant tumors in various animals and primary hepatocellular carcinoma in human populations.[57] Using AgNR SERS substrates, we can obtain high quality SERS spectra of the four AFs with different concentrations as shown in Fig. 9. The molecular structures of the four AFs are very similar, but the SERS spectra demonstrate subtle differences. Using chemometric methods such as principle component analysis (PCA) method, one can easily catalog different AFs into different group as shown in Fig. 9.

4.2 Viruses

A rapid and sensitive diagnostic method is critical for defining the emergence of a viral infection to combat public health related issues as well as threats of bioterrorism. Current diagnostic methods often have limited sensitivity, are

cumbersome, have poor predictive value, or are time-consuming. An ideal diagnostic test would not require target labeling, provide molecular specificity, and eliminate the need for an amplification step. SERS could be an ideal platform that provides the necessary level of specificity and sensitivity for biosensing. Using the AgNR SERS substrates, we show that the SERS virus spectrum provides a unique "molecular fingerprint" of individual viruses, is extremely sensitive (near single virus particle detection), is rapid (detection in 60 seconds), and does not require modification to the virus for detection.[58-60] Figure 10 shows the representative SERS spectra of influenza virus (A/HKx31), respiratory syncytial virus (RSV) (strain A2), mycroplasma (*M. pneumonia*), and human immunodeficiency virus (HIV) obtained on AgNR substrates, and the PCA method can catalog them into four well-distinguishable classes. Thus, SERS provides a framework for enhancing viral diagnostics and for evaluating anti-viral disease strategies.

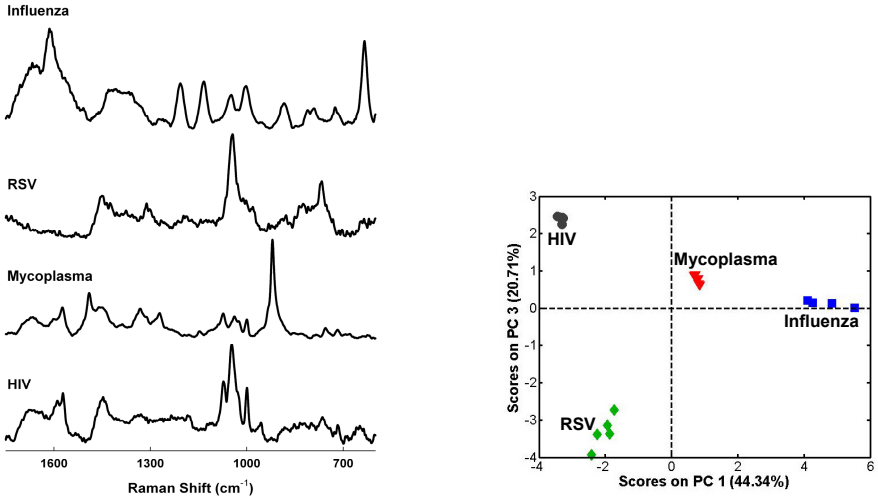

Fig. 10. The SERS spectra of four different viruses and the PCA score plot.

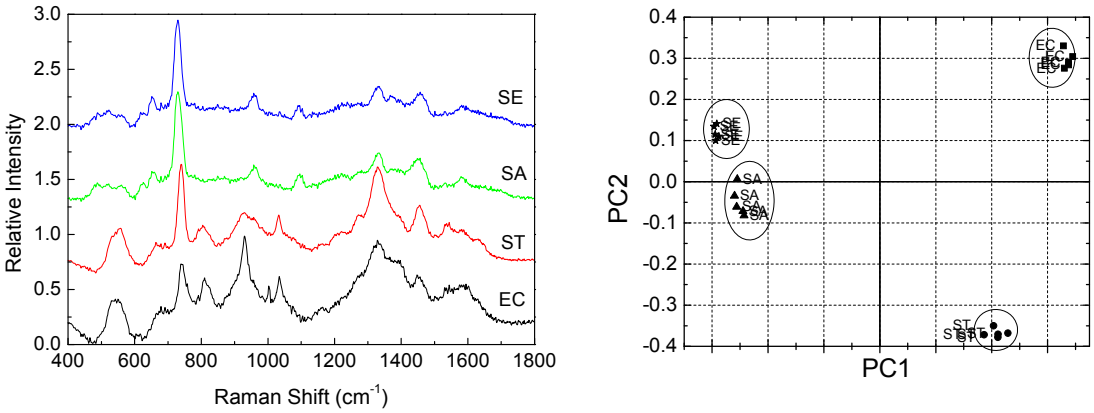

Fig. 11. The SERS spectra of four different bacteria and the PCA score plot.

4.3 Bacteria

The potential risk for deliberate contamination of the environment, food, and agricultural products has recently increased due to the global war on terrorism. Consequently, the development of portable, rapid and sensitive biosensors with on-the-spot interpretation of results is gaining momentum. From the food safety point of view, real-time microbial detection and source identification are becoming increasingly important due to the growing consumer concerns over foodborne disease outbreaks and economic loss from the outbreaks. Compared to toxins or viruses, bacteria are significantly larger. Thus bacteria have limited access to the AgNR surfaces and have less sensitivity. Nevertheless, with the AgNR SERS substrates, we have successfully detected different bacteria and differentiate them using PCA method.[61] Figure 11 shows the representative SERS spectra of four bacterial species obtained on AgNR substrates:

EC = *E. coli* O157:H7; ST = *Salmonella. typhimurium*; SA = *Staphylococcus aureus* and SE = *Staphylococcus epidermidis*. The collection time for obtaining individual spectrum was 10 s. Although the spectra look very similar, there are subtle spectral changes in wavenumber range from 600 cm^{-1} to 1200 cm^{-1}. Using the PCA method, we can also classify them into individual groups as shown in Fig. 11. This result clearly demonstrates the bacteria detection capability of AgNR substrates.

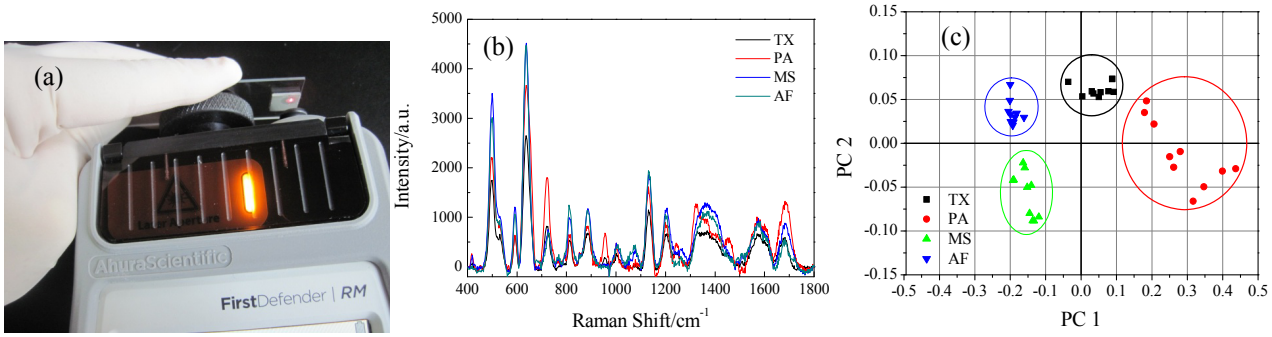

Fig. 12. (a) An picture of the handheld Raman system with an AgNR SERS substrate; (b) representative SERS spectra of three different influenza viruses and one negative control; and (c) the PCA score plot.

4.4 Hand-held detection

The combination of SERS with a handheld Raman system would lead to a powerful portable device for defense and security applications. The Thermo Scientific FirstDefender RM instrument is a 785-nm handheld Raman spectrometer intended for rapid field identification of unknown solid and liquid samples (Fig. 12(a)). It is an ideal device to integrate our AgNR substrates for portable SERS detection. This portable handheld Raman spectrometer is used, for the first time, to detect and identify three types of influenza viruses, namely Texas (TX), Pennsylvania (PA), and Mute Swan (MS), and their negative control, i.e. allantoic fluid (AF), with a multi-well AgNR SERS chip. The representative baseline-corrected SERS spectra are shown in Fig. 12(b). These SERS spectra with rich peaks demonstrate that the instrument can be used for SERS-based influenza virus detection. With the help of PCA method, these SERS spectra can be grouped into different influenza viruses/negative control as shown in Fig. 12(c). Our results demonstrate that the combination of good and reproducible SERS substrates with a portable Raman spectrometer is a powerful field device for chemical and biological sensing

5. CONCLUSIONS

In summary, we have presented an overview on current status of AgNR based SERS substrates, their optimization, potential commercialization, and applications. The SERS response of the AgNR substrates depends strongly on the length and shape of the nanorods, the deposition angle, as well as the underlayer thin film. With the unique physical vapor deposition system, those AgNR substrates can be produced with large quantity and in large area with very uniform response and high sensitivity. They can be engineered into multi-well format for high through-put screening, deposited on top of optical fibers for remote sensing, and used for on-chip separation and detection devices. We also show that the AgNR based SERS platform can be used for detection and classify toxins, viruses, and bacteria. By combing AgNR SERS substrates with a portable handheld Raman system, we demonstrate the capability to apply the small device for influenza virus detection and differentiation. All these demonstrate that AgNR based SERS substrates are powerful SERS substrates that could find extensive applications in defense and security.

Acknowledgement: The work presented here was supported by multiple grants: the National Science Foundation under the contract No. ECS-0304340, ECCS-0701787, ECCS-1029609, and CBET-1064228, US Army Research Laboratory under the contract No.W911NF-07-2-0065, W911NF-07-R-0001-04, US Army NVESD at Fort Belvoir, and US Department of Agriculture CSREES grant number 2009-35603-05001. The author would like to thank the contributions from our collaborators, Prof. R. A. Tripp, Prof. R. A. Dluhy, Prof. Y.-W. Huang, Prof. D. Krauss, and Dr. J. D. Driskell, and co-workers, Dr. J. P. Singh, Dr. Z. Y. Zhang, Dr. V. Chu, Dr. Y. J. Liu, Dr. Yu Zhu, Dr. S. Hennigan, Mr. J. Abell, Mr. X. M. Wu, and Miss J. Chen.

*zhaoy@physast.uga.edu; phone 1 706 542-7792; fax 1 706 542-2492

REFERENCES

[1] Hudson, S. and G. Chumanov, *Bioanalytical applications of SERS (surface-enhanced Raman spectroscopy).* Analytical and Bioanalytical Chemistry, 2009. **394**(3): p. 679-686.

[2] Jarvis, R.M. and R. Goodacre, *Characterisation and identification of bacteria using SERS.* Chemical Society Reviews, 2008. **37**(5): p. 931-936.

[3] Driskell, J.D., et al., *Infectious Agent Detection With SERS-Active Silver Nanorod Arrays Prepared by Oblique Angle Deposition.* Sensors Journal, IEEE, 2008. **8**(6): p. 863-870.

[4] Fleischmann, M., P.J. Hendra, and A.J. McQuillan, *Raman Spectra of Pyridine Adsorbed at a Silver Electrode.* Chem. Phys. Lett., 1974. **26**: p. 163-166.

[5] Albrecht, M.G. and J.A. Creighton, *Anomalously intense Raman spectra of pyridine at a silver electrode.* Journal of the American Chemical Society, 1977. **99**: p. 5215-5217.

[6] Jeanmaire, D.L. and R.P. Van Duyne, *Surface Raman spectroelectrochemistry. Part I. Heterocyclic, aromatic, and aliphatic amines adsorbed on the anodized silver electrode.* J. Electroanal. Chem., 1977. **84**: p. 1-20.

[7] Campion, A. and P. Kambhampati, *Surface-Enhanced Raman Scattering.* Chem. Soc. Review, 1998. **27**: p. 241-250.

[8] Otto, A., et al., *Surface enhanced Raman scattering.* J. Phys. Condens. Matt., 1992. **4**: p. 1143-1212.

[9] Cotton, T.M. and E.S. Brandt, *Surface enhanced Raman scattering*, in *Physical Methods of Chemistry*1992, Wiley: New York. p. 633-718.

[10] Moskovits, M., *Surface enhanced spectroscopy.* Rev. Mod. Phys., 1985. **57**: p. 783-826.

[11] Pemberton, J.E., *Surface enhanced Raman scattering*, in *Electrochemical Interfaces. Modern Techniques for In-Situ Characterization*, H.D. Abruna, Editor 1991, VCH Verlag Chemie: Berlin. p. 195-263.

[12] Weaver, M.J. and S. Zou, *Vibrational spectroscopy of electrochemical interfaces. Some walls and bridges to surface science understanding.*, in *Spectroscopy for Surface Science*, R.J.H. Clark and R.E. Hester, Editors. 1998, J. Wiley & Sons: Chichester, U.K. p. 219-272.

[13] Chang, R.K. and T.E. Furtak, *Surface Enhanced Raman Scattering*1982, New York: Plenum.

[14] Ruperez, A. and J.J. Laserna, *Surface Enhanced Raman Spectroscopy*, in *Modern Techniques in Raman Spectroscopy*, J.J. Laserna, Editor 1996, John WIley and Sons: Chichester, U.K. p. 227-261.

[15] Moskovits, M., *Surface-enhanced Raman spectroscopy: a brief retrospective.* J. Raman Spectros., 2005. **36**: p. 485-496.

[16] Kahl, M., et al., *Periodically structured metallic substrates for SERS.* Sensors and Actuators B-Chemical, 1998. **51**(1-3): p. 285-291.

[17] De Jesus, M.A., et al., *Nanofabrication of densely packed metal-polymer arrays for surface-enhanced Raman spectrometry.* Applied Spectroscopy, 2005. **59**(12): p. 1501-1508.

[18] Sackmann, M., et al., *Nanostructured gold surfaces as reproducible substrates for surface-enhanced Raman spectroscopy.* Journal of Raman Spectroscopy, 2007. **38**(3): p. 277-282.

[19] Billot, L., et al., *Surface enhanced Raman scattering on gold nanowire arrays: Evidence of strong multipolar surface plasmon resonance enhancement.* Chemical Physics Letters, 2006. **422**(4-6): p. 303-307.

[20] Reilly, T.H., J.D. Corbman, and K.L. Rowlen, *Vapor deposition method for sensitivity studies on engineered surface-enhanced Raman scattering-active substrates.* Analytical Chemistry, 2007. **79**(13): p. 5078-5081.

[21] Alvarez-Puebla, R., et al., *Nanoimprinted SERS-active substrates with tunable surface plasmon resonances.* J. Phys. Chem. C, 2007. **111**: p. 6720.

[22] Jensen, T.R., G.C. Schatz, and R.P. Van Duyne, *Nanosphere lithography: Surface plasmon resonance spectrum of a periodic array of silver nanoparticles by ultraviolet-visible extinction spectroscopy and electrodynamic modeling.* Journal of Physical Chemistry B, 1999. **103**(13): p. 2394-2401.

[23] Hulteen, J.C., et al., *Nanosphere lithography: Size-tunable silver nanoparticle and surface cluster arrays.* Journal of Physical Chemistry B, 1999. **103**(19): p. 3854-3863.

[24] Jensen, T.R., et al., *Nanosphere lithography: Effect of the external dielectric medium on the surface plasmon resonance spectrum of a periodic array of sliver nanoparticles.* Journal of Physical Chemistry B, 1999. **103**(45): p. 9846-9853.

[25] Jensen, T.R., et al., *Nanosphere lithography: Tunable localized surface plasmon resonance spectra of silver nanoparticles.* Journal of Physical Chemistry B, 2000. **104**(45): p. 10549-10556.

[26] Haynes, C.L. and R.P. Van Duyne, *Nanosphere lithography: A versatile nanofabrication tool for studies of size-dependent nanoparticle optics.* Journal of Physical Chemistry B, 2001. **105**(24): p. 5599-5611.

[27] Ormonde, A.D., et al., *Nanosphere lithography: Fabrication of large-area Ag nanoparticle arrays by convective self-assembly and their characterization by scanning UV-visible extinction spectroscopy.* Langmuir, 2004. **20**(16): p. 6927-6931.
[28] Zhang, X., et al., *Surface-enhanced Raman spectroscopy biosensors: excitation spectroscopy for optimisation of substrates fabricated by nanosphere lithography.* IEE Proc. Nanobiotechnol., 2005. **152**: p. 195.
[29] Haynes, C.L., et al., *Angle-Resolved Nanosphere Lithography: Manipulation of Nanoparticle Size, Shape, and Interparticle Spacing.* J. Phys. Chem. B, 2002. **106**: p. 1898-1902.
[30] Yao, J.L., et al., *A complementary study of surface-enhanced Raman scattering and metal nanorod arrays.* Pure and Applied Chemistry, 2000. **72**(1-2): p. 221-228.
[31] Kartopu, G., et al., *A novel SERS-active substrate system: Template-grown nanodot-film structures.* Physica Status Solidi a-Applications and Materials Science, 2006. **203**(10): p. R82-R84.
[32] Zhang, L.S., P.X. Zhang, and Y. Fang, *An investigation of the surface-enhanced Raman scattering effect from new substrates of several kinds of nanowire arrays.* Journal of Colloid and Interface Science, 2007. **311**(2): p. 502-506.
[33] Ruan, C.M., et al., *Controlled fabrication of nanopillar arrays as active substrates for surface-enhanced Raman spectroscopy.* Langmuir, 2007. **23**(10): p. 5757-5760.
[34] Broglin, B.L., et al., *Investigation of the effects of the local environment on the surface-enhanced Raman spectra of striped gold/silver nanorod arrays.* Langmuir, 2007. **23**(8): p. 4563-4568.
[35] Gu, G.H., et al., *Optimum length of silver nanorods for fabrication of hot spots.* Journal of Physical Chemistry C, 2007. **111**(22): p. 7906-7909.
[36] Lombardi, I., et al., *Template assisted deposition of Ag nanoparticle arrays for surface-enhanced Raman scattering applications.* Sensors and Actuators B-Chemical, 2007. **125**(2): p. 353-356.
[37] Jung, D.S., et al., *Facile fabrication of large area nanostructures for efficient surface-enhanced Raman scattering.* Journal of Materials Chemistry, 2006. **16**(30): p. 3145-3149.
[38] Walsh, R.J. and G. Chumanov, *Silver coated porous alumina as a new substrate for surface-enhanced Raman scattering.* Applied Spectroscopy, 2001. **55**(12): p. 1695-1700.
[39] Chan, S., et al., *Surface-enhanced Raman scattering of small molecules from silver-coated silicon nanopores.* Advanced Materials, 2003. **15**(19): p. 1595-+.
[40] Lin, H.H., et al., *Surface-enhanced Raman scattering from silver-plated porous silicon.* Journal of Physical Chemistry B, 2004. **108**(31): p. 11654-11659.
[41] Henley, S.J., J.D. Carey, and S.R.P. Silva, *Silver-nanoparticle-decorated carbon nanoscaffolds: Application as a sensing platform.* Applied Physics Letters, 2006. **89**(18).
[42] Chattopadhyay, S., et al., *Surface-enhanced Raman spectroscopy using self-assembled silver nanoparticles on silicon nanotips.* Chemistry of Materials, 2005. **17**(3): p. 553-559.
[43] Suzuki, M., et al., *In-line aligned and bottom-up Ag nanorods for surface-enhanced Raman spectroscopy.* Applied Physics Letters, 2006. **88**: p. 203121.
[44] Suzuki, M., et al., *Au nanorod arrays tailored for surface -enhanced Raman specroscopy.* Analytical Sciences, 2007. **23**: p. 829-833.
[45] Chaney, S.B., et al., *Aligned silver nanorod arrays produce high sensitivity surface-enhanced Raman spectroscopy substrates.* Applied Physics Letters, 2005. **87**(3).
[46] Driskell, J., et al., *The use of aligned silver nanorod arrays prepared by oblique angle vapor deposition.* J. Phys. Chem. C, 2008. **112**: p. 895-901.
[47] Liu, Y., H. Chu, and Y. Zhao, *Silver nanorod array substrates fabricated by oblique angle deposition: morphological, optical and SERS characterizations.* J. Phys. Chem. C, 2010. **114**: p. 8176-8183.
[48] Zhou, Q., et al., *The effect of underlayer thin films on the surface-enhanced Raman scattering response of Ag nanorod substrates.* Appl. Phys. Lett., 2010. **97**: p. 121902.
[49] Zhou, Q., et al., *Surface-enhanced Raman scattering from helical silver nanorod arrays.* Chem. Comm., 2011. **47**: p. 4466-4468.
[50] Zhou, Q., et al., *Optical properties and surface enhanced Raman scattering of L-shaped silver nanorod arrays.* J. Phys. Chem. C 2011. **115**: p. 14131-14140.
[51] Abell, J.L., et al., *Fabrication and characterization of a multiwell array SERS chip with biological applications.* Biosens. Bioelectron., 2009. **24**(12): p. 3663-3670.
[52] DeJesus, M.A., et al., *Nanofabrication of Densely Packed Metal-Polymer Arrays for Surface-Enhanced Raman Spectrometry.* Appl. Spectrosc., 2005. **59**(12): p. 1501-1508.

[53] Abell, J., et al., *Differentiating Intrinsic SERS spectra from a mixture by sampling induced composition gradient and independent component analysis.* Analyst 2012. **137**: p. 73-76.
[54] Zhu, Y., R.A. Dluhy, and Y.-P. Zhao, *Development of silver nanorod array based fiber optic probes for SERS detection.* Sensors & Actuators B, 2011. **157**: p. 42-50.
[55] Kurtzman, C.P., B.W. Horn, and C.W. Hesseltine, *ASPERGILLUS-NOMIUS, A NEW AFLATOXIN-PRODUCING SPECIES RELATED TO ASPERGILLUS-FLAVUS AND ASPERGILLUS-TAMARII.* Antonie Van Leeuwenhoek Journal of Microbiology, 1987. **53**(3): p. 147-158.
[56] IARC, *Aflatoxins*, in *IARC Monographs on the Evaluation of Carcinogenic Risks to Humans: Some Traditional Herbal Medicines, Some Mycotoxins, Naphthalene and Styren*2002, IARC Scientific Publication: Lyon, France. p. 9-13.
[57] Essigmann, J.M., et al., *STRUCTURAL IDENTIFICATION OF MAJOR DNA ADDUCT FORMED BY AFLATOXIN-B1 INVITRO.* Proceedings of the National Academy of Sciences of the United States of America, 1977. **74**(5): p. 1870-1874.
[58] Shanmukh, S., et al., *Rapid and sensitive detection of respiratory virus molecular signatures using surface enhanced Raman.* Nano Letters 2006. **6**: p. 2630-2636.
[59] Shanmukh, S., et al., *Identification and classification of respiratory syncytial virus (RSV) strains by surface enhanced Raman spectroscopy and multivariate statistical techniques.* Analytical and Bioanalytical Chemistry, 2008. **390**: p. 1551-1555.
[60] Driskell, J.D., et al., *Rapid and sensitive detection of Rotavirus molecular signatures using surface enhanced Raman spectroscopy.* PLoS One 2010. **5**: p. e10222.
[61] Chu, S.-Y., Y.-W. Huang, and Y.-P. Zhao, *Silver nanorod array as a SERS substrate for foodborne pathogenic bacteria detection.* Applied Spectroscopy, 2008. **62**: p. 922-931.